cDNA microarray profiling of rat cholangiocarcinoma induced by thioacetamide

CHUN-NAN YEH[1*], WEN-HUI WENG[2*], GOVINDA LENKA[2], LEE-CHENG TSAO[2], KUN-CHUN CHIANG[3], SEE-TONG PANG[4], TSUNG-WEN CHEN[1], YI-YIN JAN[1] and MIIN-FU CHEN[1]

[1]Department of Surgery, Chang Gung Memorial Hospital, Chang Gung University, Linkou 333; [2]Department of Chemical Engineering and Biotechnology, Institute of Biochemical and Biomedical Engineering, National Taipei University of Technology, Taipei 10608; [3]Department of Surgery, Chang Gung Memorial Hospital, Chang Gung University, Keelung 222; [4]Department of Urology, Chang Gung Memorial Hospital, Chang Gung University, Linkou 333, Taiwan, R.O.C.

Received January 8, 2013; Accepted May 14, 2013

DOI: 10.3892/mmr.2013.1516

Abstract. Cholangiocarcinoma (CCA) is a malignant neoplasm affecting thousands of individuals worldwide. CCA develops through a multistep process. In the current study, an oral thioacetamide (TAA)-induced model of rat CCA was established which generates the histological progression of human CCA, particularly the mass-forming type. Seven male Sprague-Dawley rats were treated with TAA for 24 weeks to induce CCA. Following the generation of the rat CCA model, whole rat genomic oligo microarray was performed to examine gene expression profiles in CCA and non-cancerous liver samples. In brief, 10,427 genes were found to be differentially expressed (8,318 upregulated and 3,489 downregulated) in CCA compared with non-tumor liver tissue. The top 50 genes (upregulated or downregulated) were selected and their functional involvement in various pathways associated with cancer progression was analyzed, including cell proliferation, apoptosis, metabolism and the cell cycle. In addition, increased expression of CLCA3, COL1A2, DCN, GLIPr2 and NID1, and decreased expression of CYP2C7 and SLC10A1 were validated by quantitative real-time PCR. Immunohistochemical analysis was performed to determine the protein expression levels of GLIPr2 and SLC10A1. The gene expression profiling performed in this study provides a unique opportunity for understanding the carcinogenesis of TAA-induced CAA. In addition, expression profiling of a number of specific genes is likely to provide important novel biomarkers for the diagnosis of CCA and the development of novel therapeutic strategies for CCA.

Correspondence to: Dr See-Tong Pang, Department of Urology, Chang Gung Memorial Hospital, Chang Gung University, Linkou 333, Taiwan, R.O.C.
E-mail: pst64lab@gmail.com

[*]Contributed equally

Key words: cholangiocarcinoma, thioacetamide, carcinogenesis, cDNA expression array, pathway analysis, diagnostic markers

Introduction

Cholangiocarcinoma (CCA) is a lethal malignancy derived from the epithelial cells (i.e. cholangiocytes) of the bile duct. CCA exhibits a considerable variety of symptoms commonly at the later stages of disease and therefore treatment for CCA is extremely difficult. CCA is grossly divided into mass forming (MF), periductal infiltrating and intraductal papillary subtypes (1). Gross pathological classifications of CCA are important in clinical practice and further translational investigations due to the distinct characteristics and outcomes following hepatectomy (2). The incidence of CCA exhibits considerable geographical variation but generally accounts for 5-30% of primary liver cancer (3). Previous studies have reported that the incidence and mortality rates of CCA have been increasing worldwide, particularly intrahepatic CCA (4-6). CCA is caused by a number of risk factors, including parasitic infections, primary sclerosing cholangitis, choledochal cysts, hepatolithiasis and carcinogen exposure, which leads to the significant variance in incidence rates of CCA worldwide (7-9).

Clinically, CCA remains extremely challenging as patients do not typically exhibit clear symptoms until the disease is quite advanced and therefore it is difficult to diagnose in its early stages. In addition to surgical treatments (2,10-14), radiation therapy and current chemotherapeutic protocols have not been found to significantly improve the long-term survival rates of CCA patients (8,15). In our previous study, a thioacetamide (TAA)-induced CCA rat model was established to analyze the molecular and morphological behavior of CCA, aiming to generate a powerful preclinical platform to provide insights into therapeutic and chemopreventative strategies for human CCA (16). Since the model recapitulates the dysplasia-carcinoma sequence of human CCA, it is likely to be crucial for the identification of the genetic basis of cholangiocellular neoplasia.

A number of previous studies have aimed to determine the molecular alterations involved in cholangiocarcinogenesis; however, these processes remain largely unknown (17-19). At present, gene expression profiling by DNA microarray represents a promising technique for understanding the molecular abnormalities involved in cancer development. In our previous study, MUC4 overexpression was identified in rat CCA (carcinogenesis caused by TAA) compared with non-tumor liver tissue (20). In the present study, a whole genome rat cDNA microarray was used to determine whether the gene expression profile for CCA reflects a specific etiological agent, with the aim to improve the understanding of the molecular events associated with CCA. In addition, this study compared the molecular profiles in non-cancerous liver to TAA-induced CCA to gain insight into changes in gene expression associated with cholangiocellular carcinogenesis and to identify potential diagnostic biomarkers. The investigation of the molecular pathophysiology associated with CCA is becoming increasingly important and necessary.

Materials and methods

Animals, treatment and CCA samples. The experimental animal ethics committee of Chang Gung Memorial Hospital (Linkou, Taiwan, R.O.C.) approved all animal protocols in this study. This study conformed to the US National Institute of Health guidelines for the care and use of laboratory animals (21). Seven adult male Sprague-Dawley (SD) rats (330-370 g) were used in these experiments. Rats were housed in an animal room under a 12:12-hour light-dark cycle (light between 08:00 a.m. and 08:00 p.m.) at an ambient temperature of 22±1˚C, with food and water available *ad libitum*. Seven experimental rats were administered 300 mg/l TAA in their drinking water daily until week 24. CCA was collected over the 24-week TAA treatment. Only CCA was used for array analysis to avoid variations in expression arising from histologically different tumor progression. Each carcinoma used in this study was obtained from a separate rat.

RNA isolation. Total RNA was isolated using TRIzol (Invitrogen Life Technologies, Carlsbad, CA, USA) according to the manufacturer's instructions. The integrity of RNA was checked using an agarose gel.

Expression array. The Whole Rat Genome oligo-microarray (P/N G4131A; Agilent Technologies, Santa Clara, CA, USA) was used for microarray experiments. RNA sample preparation for microarray analysis was performed according to the manufacturer's instructions. In brief, 20 μg total RNA was used for cyanine 3-dUTP (Cy3; test) and Cy5-dUTP (reference) labeling. Labeling was performed by oligo(dT)-primed polymerization using SuperScript II reverse transcriptase (Life Technologies, Grand Island, NY, USA) and the labeled Cy3 and Cy5 cDNA probes were purified using a Qiagen PCR QIAquick PCR Purification kit (#28104; Qiagen, Hilden, Germany). Array hybridization was performed at 60˚C for 14-16 h. Following hybridization, the array was washed and dried using the Agilent washing kit. The array image was captured using the Axon GenePix 4000 laser scanner and probe intensity was calculated with GenePix Pro 6.0 software (Molecular Devices, Sunnyvale, CA, USA). The raw data was further examined using Nexus Expression Software (BioDiscovery, Hawthorne, CA, USA).

Data processing and analysis. Microarray data analysis was performed as described previously with specific modifications (22). Image analysis was performed with GenePix Pro software. Automatic and manual flagging were used to localise absent or extremely weak spots (<2-fold higher than background), which were excluded from the analysis. The signal from each spot was calculated as the average intensity minus the average local background. Expression ratios of Cy5/Cy3 (or Cy3/Cy5 in case of dye-swap) were normalized using a method that accounts and corrects for intensity-dependent artefacts in the measurements; the LOWESS method in the SMA package. SMA is an add-on library written in the public domain statistical language, R. Three independent microarray experiments were performed. Following data normalization, genes with a 2-fold change in expression compared with the control sample were considered as differentially expressed genes between samples. All genes with a $\log_2$ ratio ≥1 or ≤-1 were considered to be statistically significant. Specific differentially expressed genes were grouped based on information from the KEGG database (23,24), NCBI, Gene Ontology and DAVID (25,26) (Tables I and II). Specific genes were annotated for several functions; however, genes were assigned to one group only (Tables I and II).

Quantitative real-time PCR (qPCR). qPCR was performed using SYBR Green Super mix (Bio-Rad, Hercules, CA, USA) in a 20 μl total volume and a Bio-Rad iCycler iQ Real-Time Detection System according to the manufacturer's instructions. Primers were designed using Beacon Designer software (Premier Biosoft International, Palo Alto, CA, USA) and are presented in Table III. PCR was performed in triplicate and relative gene expression levels in normal and tumor tissue were calculated by normalizing against β-actin expression levels using the comparative C_T method. C_T represents the cycle numbers at which the amplification reaches a threshold level selected in the exponential phase of all PCR. Data were analyzed using the iCycle iQ system software. Significance of expression difference was identified by the t-test calculator in Graph pad software (GraphPad Software, Inc., La Jolla, CA, USA).

Immunohistochemical analysis. Rat CCA tissues embedded in paraffin were cut into 5-mm sections. The sections were dewaxed in Bioclear (Bio-Optica, Milan, Italy) and rehydrated in decreasing concentrations of ethanol. Paraffin sections were pre-treated in 0.01 M citrate buffer in a microwave oven. Normal horse serum was used as a blocking agent. The sections were then incubated with antibodies against GLIpr2 (Santa Cruz Biotechnology, Inc., Santa Cruz, CA, US) and SLC10A1 (Abnova, Walnut, CA, USA). Following washing in TBS containing 0.1% Tween-20, the sections were exposed to a secondary antibody. Next, the slides were incubated with horseradish peroxidase-avidin-biotin complex (Vectastain ABC Elite; Vector Laboratories, Burlingame, CA, USA). The

Table I. Top 50 significantly upregulated genes with biological process ontologies.

Ontology	Gene ID	Gene symbol	Gene description	Fold change
Cell adhesion molecules	NM_031521	Ncam1	Neural cell adhesion molecule 1	3.92235410303046
	NM_012705	Cd4	CD4 antigen	3.85832760624149
	NM_172067	Spon1	Spondin 1	3.83860585169924
	NM_053909	Nfasc	Neurofascin	3.44243163237158
Cell death	NM_001007735	Sertad1	Serta domain-containing 1	4.75153117961431
	NM_171988	Bcl2l11	Bcl2-like 11 (apoptosis facilitator; Bcl2l11), transcript variant 3	4.34809778573906
Cell growth	AF454371	Ahnak	Ahnak-related protein	4.14343358370448
	NM_057211	Bteb1	Basic transcription element binding protein 1	3.63347765601812
	NM_199267	v-rel	V-rel reticuloendotheliosis viral oncogene homolog A (avian; Rela)	3.53615002143989
	NM_012817	Igfbp5	Insulin-like growth factor binding protein 5	3.38491249464085
Deoxyribonuclease I activity	NM_013097	Dnase1	Deoxyribonuclease I	3.8275058577354
Fibrosis	XM_342827	GliPR2	Similar to chromosome 9 open reading frame 19; 17 kD fetal brain protein (LOC362509)	4.42322128503159
	NM_031050	Lum	Lumican	3.45085666984717
Hematopoietic cell lineage	NM_001008884	RT1-Db1	RT1 class II, locus Db1	3.36846228092561
Metabolic pathways	NM_022525	Gpx3	Glutathione peroxidase 3	3.93130723332512
	NM_012879	Slc2a2	Solute carrier family 2 (facilitated glucose transporter), member 2	3.8236468641884
	NM_153300	Aldh1a3	Aldehyde dehydrogenase family 1, subfamily	3.74838767192997
	NM_175869	Plod2	Procollagen lysine, 2-oxoglutarate 5-dioxygenase 2	3.42998378780718
Neuroendocrine secretory pathway	NM_019279	Pcsk1n	Proprotein convertase subtilisin/kexin type 1 inhibitor	3.43934389253231
Neuronal differentiation	NM_053369	Tcf4	Transcription factor 4	3.35972972064775
Osteoporosis	XM_213440	COLIA1	Similar to collagen α1 (LOC287636)	3.580131772724
Protein digestion and absorption	XM_216399	LOC298069	Collagen, type XV, α1 (Col15a1)	3.33229268844969
	NM_031341	Slc7a7	Solute carrier family 7 (cationic amino acid transporter, y+ system), member 7	3.33134108780008
RNA transport	NM_017063	Kpnb1	Karyopherin (importin) β1	3.51437343518773

Table I. Continued.

Ontology	Gene ID	Gene symbol	Gene description	Fold change
Signal transduction pathways	NM_001007005	Arhgdia	Rho gdp dissociation inhibitor (GDI) α	3.9113860940851
	NM_013127	Cd38	Cd38 antigen	3.91115383379829
	NM_057116	Ppp2r2c	Protein phosphatase 2 (formerly 2A), regulatory subunit B (PR 52), γ isoform	3.40886940369163
	NM_024129	Dcn	Decorin	3.36137935471163
Structural proteins	NM_181089	Mast1	Microtubule associated serine/threonine kinase 1	4.11144062655087
Others	U06751	pSMC	Fisher 344 pre-sialomucin complex	6.57759198187846
	XM_345756	LOC366769	Similar to Ig heavy chain precursor V region (IdB5.7)	4.80829731905218
	XM_341923	LOC361644	Similar to pyruvate kinase, M1 isozyme (pyruvate kinase muscle isozyme)	4.24360287494609
	XM_225043	LOC306628	Similar to collagen α 2(IV) chain precursor	4.20372195431914
	XM_223569	LOC305482	Similar to myotubularin-related protein 3	4.15416630589892
	XM_233686	LOC313722	Similar to SPRY domain-containing SOCS box protein SSB-1	4.08502203156001
	XM_223781	LOC305679	Similar to vinculin (metavinculin)	3.90695618191964
	NM_139041	MUC-13	Putative cell surface antigen (LOC207126)	3.89086963314564
	XM_236535	LOC300920	Similar to claudin-2	3.84946284637836
	XM_214861	LOC292699	Similar to casitas B-lineage lymphoma c	3.77729841356227
	XM_223944	LOC305824	Similar to α enolase (2-phospho-D-glycerate hydro-lyase) (Non-neural enolase; NNE; Enolase 1)	3.69235152157205
	XM_242992	LOC313536	Similar to β-1,4-galactosyltransferase II	3.67034914805361
	XM_343901	LOC363605	Similar to RIKEN cDNA 2210407C18	3.66158192578579
	XM_342245	LOC361945	Similar to osteoblast specific factor 2 precursor	3.66054009489806
	XM_237497	LOC316717	Similar to protein phosphatase 1	3.60236548308193
	XM_344268	LOC364208	Similar to DKFZP566K1924 protein	3.51188899584009
	XM_214386	LOC290856	Similar to defensin 5 precursor (RD-5; Enteric defensin)	3.45619469144432
	XM_227388	LOC310614	Similar to transcription repressor p66	3.42529996437158
	XM_346200	LOC367530	Similar to RIKEN cDNA 4933431D05	3.41118393261051
	XM_243652	Plxnb2	Similar to KIAA0315 (LOC315217)	3.40547098028761
	XM_233386	LOC313499	Similar to hypothetical protein DKFZp566D1346	3.40381726129247

Table II. Top 50 significantly downregulated genes with biological process ontologies.

Ontology	Gene ID	Gene symbol	Gene description	Fold change
Bile secretion	NM_133616	Sult2a1	Hydroxysteroid preferring 2 (Sth2)	-4.9054121581746
	NM_017047	Slc10a1	Solute carrier family 10 (sodium/bile acid cotransporter family), member 1	-3.14433787788225
Cell differentiation	XM_223053	Usher syndrome 2A	Similar to usherin (LOC289369)	-6.40569654980506
Complement and coagulation cascades	NM_022257	Masp1	Mannose-binding protein associated serine protease-1	-2.85305822741612
Lipid metabolic process	NM_139192	Scd1	Stearoyl-coenzyme A desaturase 1	-3.31761447196781
	XM_341791	Sult2a2	Similar to alcohol sulfotransferase (hydroxysteroid sulfotransferase; ST; ST-60; LOC361510)	-3.18536619753157
	NM_053923	Pik3c2g	Phosphatidylinositol 3-kinase, C2 domain containing, γ polypeptide (Pik3c2g)	-3.01034237267081
	NM_144750	LOC246266	Lysophospholipase	-2.92586164948934
	NM_012737	Apoa4	Apolipoprotein A-IV	-2.84424543169138
Metabolic pathways	NM_017158	Cyp2c7	Cytochrome P450, family 2, subfamily c, polypeptide 7	-3.66306395998859
	NM_138904	Gls2	Glutaminase 2 (liver, mitochondrial)	-3.34037650319876
	NM_012540	Cyp1a1	Cytochrome P450, family 1, subfamily a, polypeptide 1	-3.32079040147379
	NM_017193	Aadat	Aminoadipate aminotransferase	-3.01966588124673
	NM_175760	Cyp4a3	Cytochrome P450, family 4, subfamily a, polypeptide 3	-2.87595624954108
	NM_017159	Hal	Histidine ammonia lyase	-2.84715718276888
	NM_053902	Kynu	kynureninase (L-kynurenine hydrolase)	-2.71604891669278
	NM_030850	Bhmt	Betaine-homocysteine methyltransferase	-2.68923042042384
	NM_031835	Agxt2	Alanine-glyoxylate aminotransferase 2 (Agxt2)	-2.64435761342884
	NM_012541	Cyp1a2	Cytochrome P450, family 1, subfamily a, polypeptide 2 (Cyp1a2)	-2.64005746673363
	NM_001013057	LOC291283	Aldo-keto reductase family 1, member C2 (Akr1c2)	-2.62748122574613
	NM_198784	Mup4	Major urinary protein 4 (Mup4)	-2.57882737786856
Olfactory transduction	NM_001000888	Olr1692	Olfactory receptor gene	-4.83343644893506
	NM_001000696	Olr1845	Olfactory receptor gene	-3.1610886895668
	NM_001000386	Olr415	Olfactory receptor gene	-2.75631096513904
Peroxisome biogenesis	NM_031587	Pxmp2	Peroxisomal membrane protein 2 (Pxmp2)	-2.79776944314083

Table II. Continued.

Ontology	Gene ID	Gene symbol	Gene description	Fold change
Signaling pathways	NM_024352	Mst1	Macrophage stimulating 1 (hepatocyte growth factor-like)	-3.01686336303489
	NM_012630	Prlr	Prolactin receptor (Prlr)	-2.78270670754098
	NM_012799	Nmbr	Neuromedin B receptor (Nmbr)	-2.72210897797388
Trypsin inhibitor	NM_152936	LOC266602	Serine peptidase inhibitor, Kazal type 1 (Spink1)	-2.72988934134003
Others	TC500715	TC500715	Unknown	-4.99924740959998
	XM_226197	LOC291810	Similar to cDNA sequence BC033409	-4.85708838735576
	XM_224106	LOC290148	Similar to T-cell receptor α chain precursor V and C regions (TRA29)-rat (fragment)	-4.47997612759399
	NM_001001799	RSEP4	Spinal cord expression protein 4	-3.92583197177519
	TC462695	TC462695	I52849 alcohol sulfotransferase	-3.75483258125134
	U33847	Gucy2g	ksGC mRNA, complete cds	-3.68824766043768
	XM_228610	LOC302446	Similar to expressed sequence AW011752	-3.59095310312283
	AY383691	AY383691	LRRGT00036 mRNA, complete cds	-3.20650059581476
	AF010442	AF010442	MARRLC7A mRNA	-3.17415725515125
	TC490222	TC490222	AB027125 aldo-keto reductase AKR1C13	-3.12591316822196
	XM_224468	LOC290458	Similar to tripartite motif-containing 52	-3.12295823834706
	XM_222983	LOC289295	Similar to putative pheromone receptor (Go-VN2)	-3.0085660426128
	XM_230584	LOC311387	Similar to CG1090-PB (Drosophila melanogaster)	-2.85086212260344
	XM_341007	LOC360734	Similar to dnaJ (Hsp40) homolog, subfamily B, member 11	-2.82980905422533
	XM_233818	LOC313840	Similar to hypothetical protein	-2.79863476103598
	XM_344625	LOC364771	Similar to aldo-keto reductase family 1 member C3 (Trans-1,2-dihydrobenzene-1,2-diol dehydrogenase) (Chlordecone reductase homolog HAKRb) (HA1753) (Dihydrodiol dehydrogenase, type I) (Dihydrodiol dehydrogenase 3; DD3)	-2.795863390899
	XM_342422	LOC362120	Similar to complement C5 precursor	-2.70059226884497
	NM_012674	Spink3	Serine peptidase inhibitor, Kazal type 3 (Spink3)	-2.67592384788853
	AY387049	AY387049	LRRGT00063	-2.65932082072998
	NM_147215	Obp3	α-2u globulin PGCL4 (Obp3)	-2.65115608927097
	XM_235065	LOC299735	Similar to hypothetical protein MGC35366 (LOC299735)	-2.64919760822929

Table III. Primer sequences used for qPCR validation.

Accession no.	Gene	Gene name	Primers (forward/reverse)	Annealing temperature (˚C)
XM_217689	Clca3	Chloride channel calcium activated 3	5'-AAG GTG GCC TAC CTC CAA GT-3' 5'-GAG AAT AGG CGA GGC TCC TT-3'	58
NM_053356	Col1a2	Procollagen, type I, α2	5'-TTG ACC CTA ACC AAG GAT GC-3' 5'-CAC CCC TTC TGC GTT GTA TT-3'	60
NM_024129	Dcn	Decorin	5'-CAA TAG CAT CAC CGT TGT GG-3' 5'-CCG GAC AGG GTT GCT ATA AA-3'	60
XM_342827	Glipr2	GLI pathogenesis-related 2	5'-GAA TGT CCC ACC TCC AAA GA-3' 5'-TCA CAG GAG ATG CTC ACA GG-3'	60
XM_213954	Nid 1	Nidogen 1	5'-CCA CCC ACA TAA GCA TAC CC-3' 5'-ACT CCC AAG GTG TTG TCA GG-3'	60
NM_017158	Cyp2c7	Cytochrome P450, family 2, subfamily c, polypeptide 7	5'-ACG GGG AGA AGT TTT CTG GT-3' 5'-TGT GCT TCC TCT TGA ACA CG-3'	60
NM_017047	Slc10a1	Solute carrier family 10 (sodium/bile acid cotransporter family), member 1	5'-GGT GCC CTA CAA AGG CAT TA-3' 5'-TGA TGA CAG AGA GGG CTG TG-3'	60
	Reference			60
	β-actin		5'-GAC AGG ATG CAG AAG GAG AT-3' 5'-CTG CTT GCT GAT CCA CAT CT-3'	

complex-binding site was visualized by 3,3'-diaminobenzidine (Vector Laboratories). Sections were counterstained with hematoxylin and dehydrated prior to mounting with Pertex (Histolab Products AB, Gothenburg, Sweden) and observed under a microscrope (Olympus, Yuan Li Instrument, Taipei, Taiwan).

Results

Systemic effects of TAA administration and tumor detection rate. No instances of TAA-induced mortality were observed during the 20-week study period. TAA-fed rats were observed to exhibit significantly lower levels of body weight gain compared with the control rats beginning at 8 weeks post-treatment. Our previous biochemical analysis revealed that levels of total protein, albumin, aspartate aminotransferase, alkaline phosphatase (ALK), bilirubin and prothrombin time (PT) were similar in both groups. According to necropsy and histological results, the incidence of TAA-induced CCA was 100% (16).

Comparative expression profiling of TAA-induced CCA and non-cancerous liver tissue. Microarray gene expression profiling identified 10,427 differentially expressed genes (8,318 for ≥2-fold upregulation, 3,489 for ≤0.5-fold downregulation) in CCA compared with the non-cancerous liver tissue. Fisher 344 pre-sialomucin complex, LOC366769 (similar to Ig heavy chain precursor V region), Serta domain-containing 1, LOC362509 (GliPR 2), Bcl2-like 11 (apoptosis facilitator), pyruvate kinase muscle isozyme (similar to pyruvate kinase, M1 isozyme) and LOC306628 were predominantly overexpressed at high levels in CCA tissues; however, usher syndrome 2A [similar to usherin (LOC289369)], TC500715, hydroxysteroid preferring 2 (sult2a1), LOC291810, olfactory receptor gene (Olr1692), LOC290148 (similar to T-cell receptor α chain precursor V and C regions (TRA29)-rat (fragment) and spinal cord expression protein 4 (RSEP4) were markedly downregulated (Tables I and II). The top 50 upregulated and downregulated genes were selected and classified based on their functional involvement as demonstrated in Tables I and II.

Association of differentially expressed genes with significant molecular processes. The top 50 genes were selected to determine their functional involvement. Molecular databases, including KEGG and NCBI, were used to identify the role of each gene with different pathways. The top most differentially expressed genes in CCA were found to play a significant role in controlling cellular metabolism (Tables I and II). Upregulated genes were largely classified in groups associated with cellular metabolism, extracellular regions and ECM organization/biosynthesis, tumorigenic cascades and other important pathways associated with liver disorders, including fibrosis. Similarly, pathway analysis was performed for downregulated genes. The majority of the downregulated genes were grouped under different pathways of various processes involved in metabolism. Specifically, Sult2a1 and Slc10a1 were classified under roles in bile secretion.

Gene expression validation by qPCR. A number of genes, including Clca3, Col1a2, Dcn, Glipr2 and Nid1 were selected from the microarray expression profile based on roles associated with liver disorders and the observed increased expression was validated. In addition, Cyp2c7 and Slc10a1 were selected to confirm significant alteration of the expression of these genes in the tumor when compared with the non-tumor liver samples. qPCR was performed using total RNA extracted from CCA tissues and normal tissue samples. β-actin was used as an internal control.

Consistent with microarray expression profiling data, Clca3, Col1a2, Dcn, Glipr2 and Nid1 were found to be upregulated in all rat tumor tissues compared with normal rat tissues (Fig. 1). However, expression of Slc10a1 and Cyp2c7 was lower in rat CCA tissues compared with normal rat tissues (Fig. 1). These expression patterns were found to be statistically significant (P<0.05).

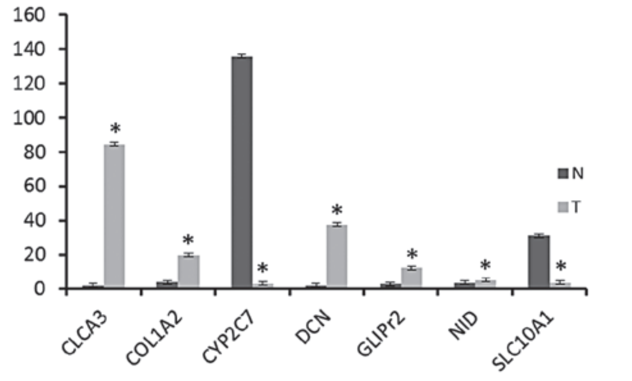

Figure 1. qPCR validation of specific differentially expressed genes identified in the expression array. Data are presented as the mean ± SD for individual gene expression changes in six paired tissue samples of N and T liver samples obtained from six rats. *P<0.05, vs N. N, normal; T, tumor; qPCR, quantitative real-time PCR.

Validation of GLIpr2 and SLC10A1 expression by immunohistochemical analysis. The mRNA expression levels of GLIpr2 and SLC10A1 were identified by microarray and qPCR analysis. To determine their protein expression in CCA tissues, immunohistochemical analysis was performed. GLIpr2 was observed as diffusely expressed in the cytoplasm and at the membrane in rat CCA samples; however, expression was absent in normal liver tissue (Fig. 2A). This observation was consistent with mRNA expression levels obtained by microarray where GLIpr2 expression was upregulated in rat CCA compared with normal liver tissue. Immunohistochemical validation was also performed for SLC10A1. However, protein expression levels were observed to be inconsistent with results obtained in the microarray; immunohistochemical analysis revealed upregulation of SLC10A1 protein levels in rat CCA compared with normal liver tissue (Fig. 2B), whereas, SLC10A1 mRNA levels were identified to be downregulated.

Discussion

CCA is a malignant neoplasm which develops through a multistep process, affecting thousands of individuals worldwide. TAA is used as a preservative for oranges; however, it is also considered to be a hepatotoxin and carcinogen, and requires metabolic activation by mixed-function oxidases (27-30). Cytochrome (CY) P450 2B, 2E1 and flavin monooxygenase metabolize TAA into its toxic metabolites (30). Previous studies have identified a number of TAA-induced liver diseases, including hyperplastic liver nodules, liver cell adenomas, hepatocarcinomas, liver cirrhosis and tumors (31-35). In our previous study, male SD rats were administered with 300 mg/l TAA in drinking water to construct an easy and reproducible animal model recapitulating the multi-stage progression of human CCA. The TAA rat model may serve as an important preclinical platform for the development of therapeutic strategies in invasive CCA and the evaluation of rational chemoprevention strategies in the dysplastic biliary epithelium. Yield of invasive CCA in the model rats was 100% at week 22 and at week 25, the yield of CCA and cirrhosis was 100% (16).

Although TAA-induced hepatic pathology is well characterized, a limited number of studies have analyzed the molecular alterations in the development of CCA. For example, alterations in the kinases, c-erb-B2 and c-met, together with possible aberrant autocrine expression of hepatocyte growth factor/scatter factor (HGF/SF), may play a significant role in the development and/or progression of human CCA (17,19,36). In addition, in our previous study the role of MUC4 as a marker of poor prognosis in mass-forming cholangiocarcinoma (MF-CCA) patients undergoing hepatectomy was investigated (20). The aim of the present study was to characterize the molecular alterations associated with TAA-induced rat CCA through cDNA microarray analysis and to identify significantly expressed genes as distinct diagnostic biomarkers for CCA. cDNA microarray analysis was used to identify the most common upregulated and downregulated genes of TAA-induced CCA. The majority of the genes were identified to play important roles in the control of various metabolic pathways.

The liver is the major drug metabolizing organ where several drug-metabolizing enzymes are present, including CYP450. CYP450 is a multi-gene family of important drug-metabolizing enzyme-encoding genes. P450 plays a key role in the metabolism of drugs, steroids, fatty acids and environmental pollutants (37). In the present microarray analysis, altered expression of members of the CYP450 family, including CYP2C7, CYP1A1, CYP4A3 and CYP1A2 (Tables I and II) was identified, consistent with the hypothesis that CYP450 family members are important for the metabolism of carcinogens. Similar to other hepatotoxins (e.g., diethylnitrosamine and carbon tetrachloride), TAA resulted in a significant reduction in the expression of CYP2C7. In agreement with previous studies (38,39), downregulation of CYP2C7 was found in male rats in the current analysis. In addition, increased expression of a number of other genes was identified, including glutathione peroxidase 3, solute carrier family 2, aldehyde dehydrogenase family 1, procollagen lysine and 2-oxoglutarate 5-dioxygenase 2, which are associated with various metabolic processes. These observations indicated that, to support the active function of cells in the CCA environment, genes involved in the metabolism of cells must be upregulated.

In addition, decreased expression of the Na^+-dependent taurocholate co-transporting protein (SLC10A1; Fig. 1) was observed, a protein responsible for the majority of hepatocellular uptake of bile salt-coupled chemotherapeutics (40). Previously,

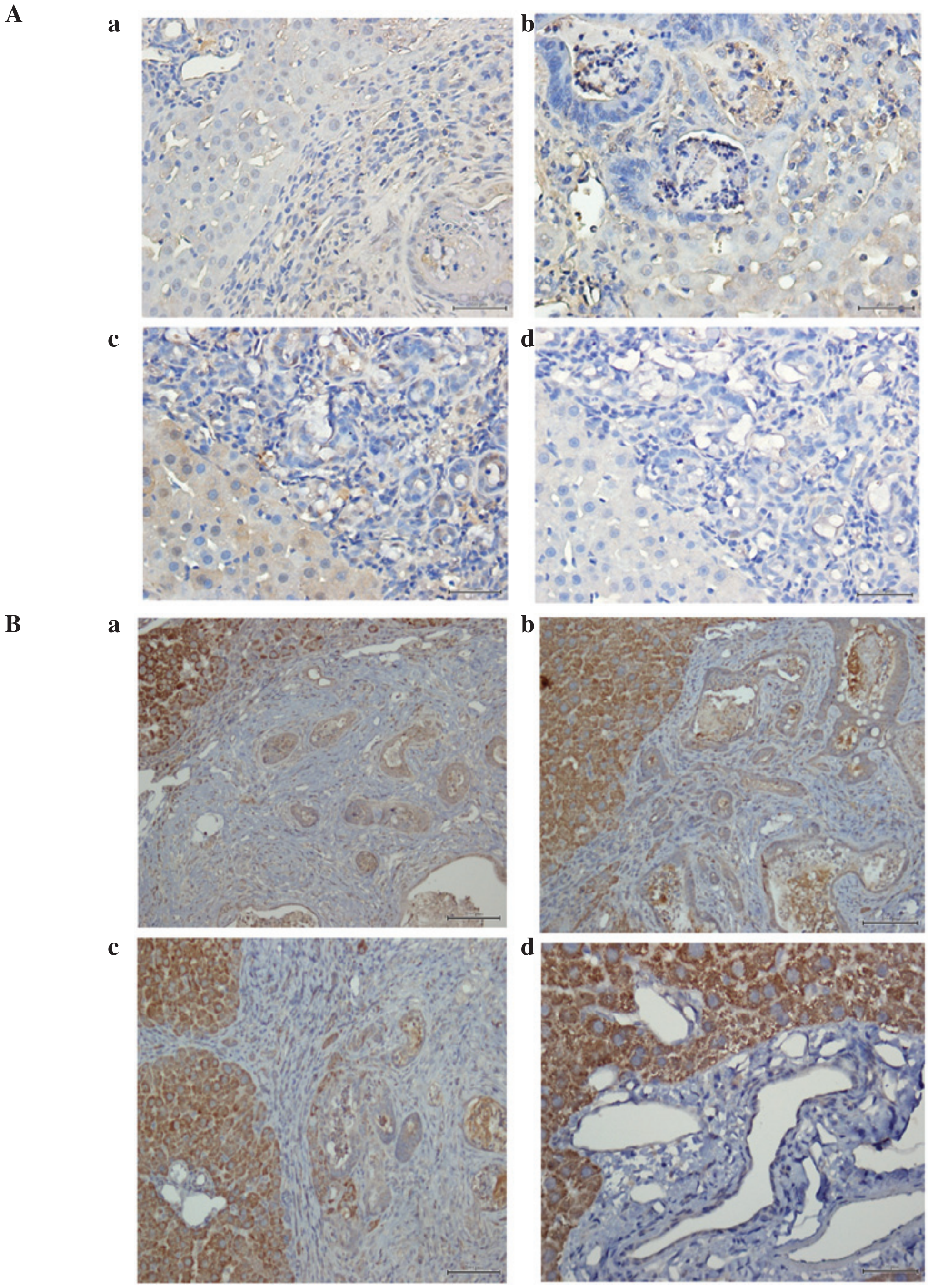

Figure 2. (A) Immunohistochemical analysis of GLIpr2 protein expression in human CCA. (Aa-c) GLIpr2 protein expression was distributed in the cytoplasm and membrane in human CCA but was absent or weak in normal hepatocytes (magnification, x200). (B) Immunohistochemical analysis of SLC10A1 protein expression in human CCA. SLC10A1 protein was downregulated and diffusely distributed in the cytoplasm and membrane in (Bd) normal liver tissue compared with (Ba-c) human CCA (magnification, x200). CCA, cholangiocarcinoma.

downregulation of Ntcp1 (Slc10a1) protein levels has been implicated in cholestasis (41). Reduced expression of Sult2a1 and Slc10a1, genes important for bile secretion (Table III), may play an important role in CCA aetiopathogenesis and those specific proteins may represent future biomarkers.

Increased expression of CLCA3, COL1A2, DCN, GLIpr2 and NID1 was further validated by qPCR (Fig. 1). DCN is a member of the small leucine-rich repeat proteoglycan family and is a major component of the extracellular matrix (42). DCN has been reported to mediate a number of functions, including proliferation, migration and differentiation of human keratinocytes by interacting with the epidermal growth factor receptor, ErbB2 (43), TGFβ (44) and cytokines. In addition to its well-known role in extracellular matrix organization, previous studies have also reported abnormal expression in a number of types of cancer, including oral cancer (45). In the present study, DCN was found to be differentially expressed in CCA, indicating its appearance and overexpression as a possible biological marker of CCA progression.

Nid is an important constituent of basement membranes, which forms a defined supramolecular complex between the extracellular matrix molecules, laminin-1 and type IV collagen (46). Previously, Nid and specific laminin chains were revealed to play a crucial role in determining the outcome of hepatic injury, in a study involving partial hepatectomy. Increased expression of Nid1 may be involved in the concomitant correlation between TAA-induced rat CCA and liver cirrhosis.

In a previous study, increased GLIpr-2 expression in the kidney was hypothesized to contribute to the development of fibrosis by increasing the pool of activated fibroblasts, possibly through the induction of epithelial-mesenchymal transition (47). The biological function of GLIpr-2 remains poorly understood. The enhanced expression of GLIpr-2 in TAA-induced CCA may play a pivotal role in liver fibrosis and represent an additional molecular target which must be analyzed further.

In conclusion, the extensive information gained from the gene expression profiling of TAA-induced CCA performed in the present study is likely to provide important insights into the genes involved in the development of CCA. Further studies must be performed to develop a further understanding of the cellular activities of differentially expressed genes during CCA progression.

Acknowledgements

The present study was supported by grants from the Chang Gung Medical Research Program (no. CMRPG3B0531, CMRPG3B0532, CMRPG3B0361 and CMRPG3B0362).

References

1. Liver Cancer Study Group of Japan: Classification of Primary Liver Cancer. 1st English edition. Kanehara Press Co., Tokyo, 1997.
2. Yeh CN, Yeh TS, Chen TC, Jan YY and Chen MF: Gross pathological classification of peripheral cholangiocarcinoma determines the efficacy of hepatectomy. J Gastroenterol: Sep 25, 2012 (Epub ahead of print).
3. Chen MF: Peripheral cholangiocarcinoma (cholangiocellular carcinoma): clinical features, diagnosis and treatment. J Gastroenterol Hepatol 14: 1144-1149, 1999.
4. Shaib YH, Davila JA, McGlynn K and El-Serag HB: Rising incidence of intrahepatic cholangiocarcinoma in the United States: a true increase? J Hepatol 40: 472-477, 2004.
5. Patel T: Worldwide trends in mortality from biliary tract malignancies. BMC Cancer 2: 10, 2002.
6. Chang KY, Chang JY and Yen Y: Increasing incidence of intrahepatic cholangiocarcinoma and its relationship to chronic viral hepatitis. J Natl Compr Canc Netw 7: 423-427, 2009.
7. Shaib Y and El-Serag HB: The epidemiology of cholangiocarcinoma. Semin Liver Dis 24: 115-125, 2004.
8. DeGroen PC, Gores GJ, LaRusso NF, Gunderson LL and Nagorney DM: Biliary tract cancers. N Engl J Med 341: 1368-1378, 1999.
9. Albores-Saavedra J, Henson DE and Sobin LH: The WHO histological classification of tumors of the gallbladder and extrahepatic bile ducts. A commentary on the second edition. Cancer 70: 410-414, 1992.
10. Weber SM, Jarnagin WR, Klimstra D, DeMatteo RP, Fong Y and Blumgart LH: Intrahepatic cholangiocarcinoma: resectability, recurrence pattern and outcomes. J Am Coll Surg 193: 384-391, 2001.
11. Uenishi T, Hirohashi K, Kubo S, *et al*: Histologic factors affecting prognosis following hepatectomy for intrahepatic cholangiocarcinoma. World J Surg 25: 865-869, 2001.
12. Jarnagin WR, Fong Y and DeMatteo RP: Staging, resectability and outcome in 225 patients with hilar cholangiocarcinoma. Ann Surg 234: 507-519, 2001.
13. Patel T: Increasing incidence and mortality of primary intrahepatic cholangiocarcinoma in the United States. Hepatology 33: 1353-1357, 2001.
14. Shirabe K, Shimada M and Harimoto N: Intrahepatic cholangiocarcinoma: Its mode of spreading and therapeutic modalities. Surgery 131: S159-S164, 2002.
15. Bathe OF, Pacheco JT and Ossi PB: Management of hilar bile duct carcinoma. Hepatogastroenterology 48: 1289-1294, 2001.
16. Yeh CN, Maitra A, Lee KF, Jan YY and Chen MF: Thioacetamide-induced intestinal-type cholangiocarcinoma in rat: an animal model recapitulating the multi-stage progression of human cholangiocarcinoma. Carcinogenesis 25: 631-636, 2004.
17. Terada T, Nakanuma Y and Sirica AE: Immunohistochemical demostration of MET overexpression in human intrahepatic cholangiocarcinoma and in hepatolithiasis. Hum Pathol 29: 175-180, 1998.
18. Endo K, Yoon BI, Pairojkul C, Demetris AJ and Sirica AE: ERBB-2 overexpression and cyclooxygenase-2 up-regulation in human cholangiocarcinoma and risk conditions. Hepatology 36: 439-450, 2002.
19. Hansel DE, Rahman A, Hidalgo M, *et al*: Identification of novel cellular targets in biliary tract cancers using global gene expression technology. Am J Pathol 163: 217-229, 2003.
20. Yeh CN, Pang ST, Wu RC, Chen TW, Jan YY and Chen MF: Prognostic value of MUC4 for mass-forming intrahepatic cholangiocarcinoma after hepatectomy. Oncol Rep 21: 49-56, 2009.
21. National Institutes of Health: Guide for the Care and Use of Laboratory Animals. NIH publication no. 85-23, revised 1996.
22. Pang ST, Dillner K, Wu X, Pousette A, Norstedt G and Flores-Morales A: Gene expression profiling of androgen deficiency predicts a pathway of prostate apoptosis that involves genes related to oxidative stress. Endocrinology 143: 4897-906, 2002.
23. Kanehisa M, Goto S, Sato Y, Furumichi M and Tanabe M: KEGG for integration and interpretation of large-scale molecular datasets. Nucleic Acids Res 40: D109-D114, 2012.
24. Kanehisa M and Goto S: KEGG: Kyoto encyclopedia of genes and genomes. Nucleic Acids Res 28: 27-30, 2000.
25. Huang DW, Sherman BT and Lempicki RA: Systematic and integrative analysis of large gene lists using DAVID bioinformatics resources. Nature Protoc 4: 44-57, 2009.
26. Huang DW, Sherman BT and Lempicki RA: Bioinformatics enrichment tools: paths toward the comprehensive functional analysis of large gene lists. Nucleic Acids Res 37: 1-13, 2009.
27. Dasgupta A, Chatterjee R and Chowdhury JR: Thioacetamide-induced hepatocarcinoma in rat. Oncology 38: 249-253, 1981.
28. Fitzhugh OG and Nielson AA: Liver tumors in rats fed thiourea or thioacetamide. Science 108: 626-628, 1948.
29. Al-Bader AA, Mathew TC, Abul H, Al-Mosawi M, Panigrahi D and Dashti HM: Bacterial translocation in thioacetamide induced liver cirrhosis. J R Coll Surg Edinb 43: 278-82, 1998.
30. Lee JW, Shin KD, Lee M, *et al*: Role of metabolism by flavin-containing monooxygenase in thioacetamide-induced immunosuppression. Toxicol Lett 136: 163-172, 2003.
31. Dashti H, Jeppsson B, Hagerstrand I, *et al*: Early biochemical and histological changes in rats exposed to a single injection of thioacetamide. Pharmacol Toxicol 60: 171-174, 1987.
32. Gallagher CH, Gupta DN, Judah JD and Rees KK: Biochemical changes in acute thioacetamide intoxication. J Path Bact 72: 193-201, 1956.
33. Gupta DN: Acute changes in the liver after administration of thioacetamide. J Pathol Bacteriol 72: 183-192, 1956.
34. Muller D, Zimmerman SI and Schiller F: Drug metabolism in rat liver injured by thioacetamide. Arch Toxicol 5: 368-371, 1982.
35. Dashti HM, Mathew TC, Jadaon MM and Ashkanani E: Zinc and liver cirrhosis: biochemical and histopathologic assessment. Nutrition 13: 206-212, 1997.
36. Sirica AE, Lai GH and Zhang Z: Biliary cancer growth factor pathways, cyclo-oxygenase-2 and potential therapeutic strategies. J Gastroenterol Hepatol 16: 363-372, 2001.
37. Nelson DR, Zeldin DC, Hoffman SM, Maltais LJ, Wain HM and Nebert DW: Comparison of cytochrome P450 (CYP) genes from the mouse and human genomes, including nomenclature recommendations for genes, pseudogenes and alternative-splice variants. Pharmacogenetics 14: 1-18, 2004.
38. Henderson CJ, Russell AL, Allan JA and Wolf CR: Sexual differentiation and regulation of cytochrome P-450 CYP2C7. Biochim Biophys Acta 1118: 99-106, 1992.
39. Arun KA and Bernard HS: Latent overexpression of hepatic CYP2C7 in adult male and female rats neonatally exposed to phenobarbital: a developmental profile of gender-dependent P450s. J Pharmacol Exp Ther 293: 1027-1033, 2000.
40. Hagenbuch B, Stieger B, Foguet M, Lübbert H and Meier PJ: Functional expression, cloning and characterization of the hepatocyte Na^+/bile acid cotransport system. Proc Natl Acad Sci USA 88: 10629-10633, 1991.

41. Trauner M, Meier PJ and Boyer JL: Molecular regulation of hepatocellular transport systems in cholestasis. J Hepatol 31: 165-178, 1999.
42. Kjellén L and Lindahl U: Proteoglycans: structures and interactions. Annu Rev Biochem 60: 443-475, 1991.
43. Santra M, Eichstetter I and Iozzo RV: An anti-oncogenic role for decorin. Downregulation of ErbB2 leads to growth suppression and cytodifferentiation of mammary carcinoma cells. J Biol Chem 275: 35153-35161, 2000.
44. Zhang Z, Li XJ, Liu Y, Zhang X, Li YY and Xu WS: Recombinant human decorin inhibits cell proliferation and downregulates TGF-beta1 production in hypertrophic scar fibroblasts. Burns 33: 634-641, 2007.
45. Abhijit GB, Indraneel B, William ML and Jamboor KV: Aberrant expression and localization of decorin in human oral dysplasia and squamous cell carcinoma. Cancer Res 63: 7769-7776, 2003.
46. Pujuguet P, Simian M, Liaw J, Timpl R, Werb Z and Bissell MJ: Nidogen-1 regulates laminin-1-dependent mammary-specific gene expression. J Cell Sci 113: 849-858, 2000.
47. Baxter RM, Crowell TP, George JA, Getman ME and Gardner H: The plant pathogenesis related protein GLIPR-2 is highly expressed in fibrotic kidney and promotes epithelial to mesenchymal transition in vitro. Matrix Biol 1: 20-29, 2007.